Forest Ecology and Management 619 (2026) 124135

Contents lists available at ScienceDirect

Forest Ecology and Management

journal homepage: www.elsevier.com/locate/foreco

Biophysical drivers of mountain pine beetle outbreaks in lodgepole pine forests in the Intermountain West, U.S.☆

Jackson P. Audley [a,b,*], Andrew M. Latimer [a], Christopher J. Fettig [b], A. Steven Munson [c,1], Justin B. Runyon [d], Leif A. Mortenson [e], Brytten E. Steed [f,1], Kenneth E. Gibson [f,1], Carl L. Jørgensen [g], Stephen R. McKelvey [b], Joel D. McMillin [h,1], José F. Negrón [i]

[a] Department of Plant Sciences, University of California, One Shields Avenue, Davis, CA 95616, USA
[b] Pacific Southwest Research Station, USDA Forest Service, 221 West Court Street Suite 3B, Woodland, CA 95695, USA
[c] Forest Health Protection, USDA Forest Service, 4746 South 1900 East, Ogden, UT 84403, USA
[d] Rocky Mountain Research Station, USDA Forest Service, 1648 South 7th Avenue, Bozeman, MT 59717, USA
[e] Pacific Southwest Research Station, USDA Forest Service, 2480 Carson Road, Placerville, CA 95667, USA
[f] Forest Health Protection, USDA Forest Service, 26 Fort Missoula, Missoula, MT 59804, USA
[g] Forest Health Protection, USDA Forest Service, 1249 South Vinnell Way, Suite 200, Boise, ID 83709, USA
[h] Forest Health Protection, USDA Forest Service, 2500 South Pine Knoll Drive, Flagstaff, AZ 86001, USA
[i] Rocky Mountain Research Station, USDA Forest Service, 240 West Prospect Road, Fort Collins, CO 80526, USA

ARTICLE INFO

Keywords:
Dendroctonus ponderosae
Generalized linear mixed effects models
Pinus contorta
Quadratic mean diameter
Tree size
Water availability

ABSTRACT

Mountain pine beetle, *Dendroctonus ponderosae* Hopkins, is among the most significant forest insect pests, particularly in lodgepole pine, *Pinus contorta* Dougl. ex Loud., forests in western North America. We established a network of 125, 0.081-ha circular plots in *P. contorta* forests in Colorado, Idaho, Montana, Utah, and Wyoming to document tree mortality and stand-level responses to *D. ponderosae* outbreaks. We found notable reductions in several key metrics but also observed significant variability in per-year (0–71%) and cumulative mortality (2–87%). We used this long-term monitoring dataset and employed generalized linear mixed effects modeling to determine the biophysical drivers of the variation in *P. contorta* mortality. Models were fitted to the entire (2005–2024) dataset, and to two truncated datasets: outbreak years only (2005–2012) and maximum per year *P. contorta* mortality per plot. Explanatory variables included tree, plot, and environmental factors (temperature and water availability). Our models highlighted several significant drivers of *P. contorta* mortality. The most significant and consistent were individual tree dbh and quadratic mean diameter (QMD). Larger individual tree dbh and larger QMD positively influenced the probability of *P. contorta* mortality. Tree dbh interacted significantly with water availability variables, particularly November-March snowpack. Increased snowpack and greater densities of nonhost tree species decreased mortality. These results suggest that management efforts should account for the frequency of large-diameter *P. contorta* and that density reduction and/or increasing tree species (nonhost) and structural diversity may provide mitigation strategies for reducing *P. contorta* mortality attributed to *D. ponderosae* in the Intermountain West.

1. Introduction

Native bark beetles (Coleoptera: Curculionidae) are an important component of healthy forests and influence nutrient cycling, stand dynamics, hydrology, and disturbance regimes (Morris et al., 2018). While the vast majority of the ~550 bark beetle species native to North America are not considered pest species, a subset including the mountain pine beetle, *Dendroctonus ponderosae* Hopkins, can cause landscape-level disturbances (Safranyik and Wilson, 2006; Negrón and Fettig, 2014; Fettig et al., 2022). In recent decades, tree mortality attributed to bark beetles in conifer forests of western North America has been substantial (Fettig et al., 2022); even outpacing the total area

☆ This article was written and prepared by U.S. Government employees on official time and it is, therefore, in the public domain and not subject to copyright.

* Correspondence to: Forest Ecology and Management, Department of Plant Sciences, University of California, One Shields Ave, Davis, CA 95616, USA.
E-mail address: jpaudley@ucdavis.edu (J.P. Audley).

[1] (retired)

https://doi.org/10.1016/j.foreco.2026.124135
Received 20 May 2026; Received in revised form 15 July 2026; Accepted 27 July 2026
Available online 3 August 2026

impacted by wildfires in some years (Hicke et al., 2016). *Dendroctonus ponderosae* has been a significant contributor causing mortality on > 27 million ha in western North America since 2000, with peak mortality in the western U.S. affecting > 3.5 million ha in 2009 (Fettig et al., 2022). Mortality was dominated by a regional outbreak in the Intermountain West from 2004 to 2012 (Audley et al., 2020). While *D. ponderosae* colonizes at least 15 *Pinus* spp., *P. contorta* is a preferred, economically and ecologically important host species (Negrón and Fettig, 2014).

Several factors are known to contribute to bark beetle outbreaks. At the most fundamental level, host defenses determine bark beetle colonization success, where healthy, well-defended trees are capable of fending off attacks (Raffa and Berryman, 1982). A primary driver of conifer defensive capabilities is water availability. Water limited trees typically have a reduced capacity to produce secondary metabolites (Herms and Mattson, 1992). Drought is a common occurrence in western forests (Clark et al., 2016). Increasing temperatures, coupled with an increasing occurrence and severity of droughts in some locations, are well recognized as important inciting factors for bark beetle outbreaks (Raffa et al., 2008; Bentz et al., 2010; Preisler et al., 2012; Creeden et al., 2014; Kolb et al., 2016). Another factor that influences bark beetle outbreaks and often interacts with water availability is tree density, generally via competition. Strong, positive relationships between tree density and beetle-driven tree mortality have been reported for *D. ponderosae* (Fettig et al., 2007; Hansen et al., 2023; Francis et al., 2025) and several other bark beetle systems (Negrón et al., 2009; Gaylord et al., 2013; Koontz et al., 2021; Francis et al., 2025). Recent modeling-based studies have shed light on numerous factors that influence *D. ponderosae* outbreaks (e.g., Preisler et al., 2012; Creeden et al., 2014; Francis et al., 2025; Cooke et al., 2026). Most studies have focused on relatively limited spatial and/or temporal scales. Investigation of larger datasets encompassing greater spatial and temporal scales, similarly to Hansen et al. (2023), may provide additional insights to this system. Several important pest species of *Dendroctonus* prefer to colonize large-diameter, mature trees (Six and Bracewell, 2015). This is particularly true for *D. ponderosae* in lodgepole pine, *P. contorta* Dougl. ex Loud., forests (Fettig et al., 2007; Negrón and Fettig, 2014). In response to ecological concerns over the widespread, regional *D. ponderosae* outbreaks, we installed a network of 125, 0.081-ha circular plots in *P. contorta* forests in Colorado, Idaho, Montana, Utah, and Wyoming (Audley et al., 2020). The initial goal was to describe variations in the levels of *P. contorta* mortality and stand-level responses to the outbreak. We documented significant changes in several stand characteristics including: 5% reduction in mean diameter at breast height (dbh); nearly 9% reduction in quadratic mean diameter (QMD), 16% reduction in mean tree height, 41% reduction in mean number of stems, and 52% and 53% reductions in stand density index (SDI) and basal area, respectively (Audley et al., 2020). We observed considerable variability in plot-level responses. Per year, per plot mortality of *P. contorta* averaged 5.3 ± 0.3% and ranged from 0 to 71%, while cumulative (2004–2012) per plot mortality of *P. contorta* averaged 34.8 ± 0.02% and ranged from 1.9 to 87% (Audley et al., 2020).

The objective of this study was to investigate biophysical characteristics that influenced the probability of *P. contorta* mortality across our plot network. Our work expands on recent *D. ponderosae* modeling efforts by leveraging long-term (~20 years) observational data across a large geographic area. We expected several individual tree, plot, and environmental variables would explain the variation in *P. contorta* mortality. Given recently reported results from similar modeling approaches in closely related systems (Koontz et al., 2021; Hansen et al., 2023), we hypothesized that larger tree size (particularly diameter), greater tree density, reduced water availability (i.e., increased water stress), and interactions among these variables would be positively correlated with levels of *P. contorta* mortality. Additionally, we expected seasonal weather and climate influences to differ and to see a pronounced temporal lag of water availability influence on *D. ponderosae*-caused tree mortality. Finally, we predicted that modeling different cases of the dataset would reveal different explanatory variables as the most influential, drivers of the observed *P. contorta* mortality.

2. Materials and methods

2.1. Field data collection

We determined levels of tree (all species) mortality and causal agent (s) of tree mortality from 2005 to 2024 on a network of 125, 0.081-ha, circular plots in Colorado, Idaho, Montana, Utah, and Wyoming ($n = 25$ state^{-1}). Plots were initially installed and monitored to quantify and characterize forest responses to major *D. ponderosae* outbreaks (*see* Audley et al., 2020). All plots were > 50% *P. contorta* by basal area with at least 10 *P. contorta* > 13.9 cm dbh with evidence of at least two trees colonized or killed by *D. ponderosae* within three years of plot establishment in 2010. Plots meeting these criteria were randomly selected in groups of five, with plots within groups separated by ≥ 100 m. Within each state, groups were separated by > 1.6 km (mean distance ± SEM = 23.4 ± 3.0 km). All tree species ≥ 7.62 cm diameter at breast height (dbh, 1.37 m in height) were identified, tagged, and monitored annually. For *P. contorta* killed prior to 2010, we back-dated mortality through 2005 based on the color of faded needles and degree of needle and twig retention as described by Klutsch et al. (2009) and widely used elsewhere. While this method has been widely implemented, there may have been unaccounted factors that obscured our ability to accurately ascribe the actual year of mortality. For example, a given tree may have lost needles faster than normal, resulting in an inaccurate year of death for trees killed 2005 through 2009. Despite some uncertainty inherent to this method, we were fairly confident in our ability to accurately categorize year of mortality for most trees in the dataset. *Pinus contorta* that died prior to 2005 were ignored as we could not reliably discern the year of death among trees killed in 2004 or prior.

Fifty-two plots (42%) were lost to wildfires or woodcutting over the duration of our study. While this is a significant amount, a majority of plots lost (47 of 52) were lost following the conclusion of the outbreaks across the study area, thus limiting the impact plot losses likely had on the dataset from the most critical observation window. That said, these losses of observations from the dataset may have confounded the influence of some of the explanatory variables in our final models. Wildfires burned five plots in Idaho in 2012, an additional 10 plots in Idaho in 2017, 19 plots in Colorado in 2020, and the remaining 10 plots in Idaho in 2024. Eight plots were lost to wood cutting 2015–2020 in Wyoming and Montana. Data from these 52 plots were retained for analyses through the last year of measurement (prior to the disturbance) and then were dropped from further analyses.

Causal agents of tree mortality were determined by removing ~625 cm^2 of bark with a hatchet on the north and south faces of the tree bole at ~1.7 m in height. Bark sections were investigated for bark beetle galleries. The shape, distribution, and orientation of galleries are commonly used to distinguish among bark beetle species (Furniss and Carolin, 1977). Mortality was attributed to *D. ponderosae* when *D. ponderosae* galleries were present, despite other contributing factors. For a comprehensive summary of all (15) contributing factors, see Audley et al. (2020).

2.2. Biophysical drivers and dataset creation

Using plot measurements, we created a dataset of tree and environmental variables summarized at the plot level (Table 1). Tree mortality was assessed annually and dbh and height were measured in 2010, 2014, 2018, and 2022. Among others, these data were used to estimate basal area (m^2 ha^{-1}), stand density index (SDI), QMD (cm), number of live trees ha^{-1}, number of live *P. contorta* ha^{-1}, and number of nonhost trees ha^{-1}. We estimated *D. ponderosae* "pressure" for each time step (except for 2005 as we could not differentiate between *P. contorta* killed

Table 1
Variables investigated as potential drivers of observed levels of *Pinus contorta* mortality attributed to *Dendroctonus ponderosae* in the Intermountain West, U.S., 2005–2024.

Variable Name	Definition	Range
Tree variables		
Individual tree diameter	dbh of each pine ≥ 7.62 cm	7.62–88.9 cm
Individual tree height	height of each pine ≥ 7.62 cm	2.3–30.5 m
Plot variables		
Aspect	Converted to "northern-ness" (−0.99–1 scale) by cosine transformation	−1–1
Slope	Percent slope	1–43%
Elevation	elevation at plot center	1918.6–2991.2 m
Dbh	Average dbh of all plot trees ≥ 7.62 cm	13.4–31.1 cm
Stand variables		
Total basal area (BA) ha^{-1}	basal area of all trees ≥ 7.62 cm	1.8–78.1 m^2 ha^{-1}
Number of pines ha^{-1}	Number of all pines ≥ 7.62 cm	49.4–3768.4 ha^{-1}
Number of nonhosts ha^{-1}	Number of all non-pines ≥ 7.62 cm	0–1223.2 ha^{-1}
Quadratic mean diameter (QMD)	Weighted mean of average dbh for a stand	6.9–53.4 cm
Stand density index (SDI)	Measure of tree density relating number of trees ha^{-1} to QMD	37.5–1705.4
***Dendroctonus ponderosae* pressure**		
MPB pressure	Proportion of pines killed the prior year per plot	0–0.71
Temperature		
Year average	Temperature data was averaged (for each category) from 800-m resolution PRISM data	0.65–5.89 °C
Nov-Mar average	Seasonal splits, November-March and April-August. Seasonal splits were	−9.48– −1.1 °C
Apr-Aug average	investigated for temperature and water balance variables (below)	6.58–12.42 °C
Previous year average		0.65–5.89 °C
Previous Nov-Mar		−9.0– −1.1 °C
Previous Apr-Aug		6.58–12.42 °C
Water balance variables		
Water storage	Data from NASA's GLDAS−2.1 Noah land surface model run in the ESRI Water Balance app. Average annual change in water storage; water storage is a value calculated monthly based on runoff + soil moisture + precipitation + evapotranspiration + snowpack	−17–22.83
Water storage previous year	Average annual water storage prior year	−17–22.83
Water storage 3 years prior	Average annual water storage 3 years prior	−17–22.83
Water storage Nov-Mar	Averages based on season splits (described above)	−6–153.2
Water storage Apr-Aug		−129.83–16.17
Water storage Nov-Mar prior year		−6–153.2
Water storage Apr-Aug prior year		−129.83–16.17
Water storage Nov-Mar 3 years prior		−6–153.2
Water storage Apr-Aug 3 years prior		−129.83–16.17
Water storage component variables	Variables from Noah land surface model; each variable was averaged per year, previous year, and three years prior, with seasonal splits for each time range as outlined previously	
Runoff	Amount of water not absorbed into the soil	0–136.33 mm
Soil moisture	Estimated amount of water available for uptake in the soil	150.17–619.5 mm
Precipitation	Amount of rainfall or snowfall	16.17–154.4 mm
Evapotranspiration	Estimated amount of water transferred to the atmosphere via evaporation or as a product of plant photosynthesis/respiration	23.5–105.83 mm
Snowpack	Depth of snow	0.17–111.83 mm

in 2004 and before 2004 based on crown conditions) by calculating the proportion of *P. contorta* killed by *D. ponderosae* the previous year for each plot, following a similar approach used by Hansen et al. (2023). Elevation, percent slope, and aspect were included in the dataset. For aspect, we transformed azimuth to a measure of "northern-ness" by taking the cosine of each such that 0° = 1, 90° = −0.5, 180° = 0, and 270° = 0.5.

Environmental data primarily consisted of temperature and water availability-related variables. Temperature was derived from 800-m resolution PRISM data (https://www.prism.oregonstate.edu/). Monthly temperatures were used to calculate annual and seasonal averages for both current and prior years. Breakdowns were November (prior calendar year)-March and April-August following Hansen et al. (2023) for bark beetles in ponderosa pine, *P. ponderosa* Dougl. ex Laws., forests in the Colorado Plateau, U.S. Water availability-related variables were derived from NASA's Global Land Data Assimilation System (GLDAS−2.1) inputs for the Noah land surface model through the ESRI Water Balance App (https://livingatlas.arcgis.com/waterbalance/). Data from GLDAS are calculated every three hours and aggregated into monthly averages at a ~30-km resolution. Variables included a change in water storage value, soil moisture, runoff, evapotranspiration, precipitation, and snowpack. For each variable, we calculated annual and seasonal averages for the current year (respective of each time step), previous year, and for the prior three years.

2.3. Model selection and analyses

Our dataset was comprised of 124,584 observations of 11,150 *P. contorta*. For plots that were compromised (e.g., lost due to wildfires) prior to the conclusion of the study, only observations through the final year of reliable data were included, after which those missing observations were subsequently ignored. We conducted analyses using the R statistical program (v. 4.5.1) (R Core Team, 2024). We used generalized linear mixed modeling to account for repeated measures. Models were fitted with the *glmmTMB()* function (glmmTMB package) with a tree-level, Bernoulli response (where alive = 0, dead = 1), a binomial distribution with a logit link, while controlling for repeated measures and response errors by including either plot or cluster (group of five plots within a state) and year as crossed random effects. Alternative random-effects structures were considered including state and

autoregressive lag yr^{-1} for each model; however, alternative structures did not improve model fits and were thus ignored.

All fixed effects were scaled prior to analyses to account for large differences among scales inherent to the explanatory variables in this study. Factors were initially inspected using scatter plots and collinearity was checked using Pearson's correlation coefficients. Model fits were assessed by examining the QQ and DHARMa residuals plots (DHARMa package), by pseudo R^2 values (*performance::r2()* function in the performance package), and by checking for multicollinearity using variance inflation factor (VIF) scores from the *check_collinearity()* function (performance package). Model selections were made based on model fit and by comparing Akaike Information Criterion (AIC), Bayesian Information Criterion (BIC), deviance values, and likelihood ratio tests between models. Fixed effects were systematically tested with the primary goal of optimizing the AIC value for the final models (Zuur et al., 2009). Our system of testing fits of fixed effects employed a primarily stepwise forwards selection with a stepwise backwards approach mixed in. For each model, we began adding the higher order variables (e.g., annual average temperature before seasonal averages; water storage before the individual components) in a stepwise forward selection followed by testing the corresponding lower order components to each higher order variable (when applicable) using stepwise backwards selection. For example, we fitted using annual water storage first and then fitted the same model replacing water storage with the five components (Table 1) that are used to calculate water storage, systematically removing one component at a time. This primarily forward selection with a targeted backwards selection approach allowed for an efficient exploration of the large number of explanatory variables where several variables were nested within a higher order variable. All variables from Table 1 were considered for each of the models. Highly correlated variables from our initial Pearson's correlations were swapped out in subsequent iterations rather than added to the prior fit. We considered interaction terms between several fixed effects with particular focus on interactions between tree diameter, tree density, and water stress based on studies of bark beetles in *P. ponderosa* and mixed-conifer forests in the Sierra Nevada, California (Koontz et al., 2021).

In addition to the all-years model (2005–2024), we considered two additional cases: "outbreak years only" and "maximum mortality" (i.e., maximum per year *P. contorta* mortality per plot). For outbreak years only, we restricted data to 2005–2012 (Fig. 1) a time period that captured the rise, peak, and decline of *P. contorta* mortality across study plots. The outbreak years only dataset included 66,522 observations of 11,150 *P. contorta*. For the maximum mortality model, we filtered the dataset to only include observations from the year in which the greatest proportion of *P. contorta* were killed by *D. ponderosae* for each plot. The resulting dataset for the maximum mortality model included 9766 observations of 9766 *P. contorta*. Here we were interested in isolating factors associated with the greatest, per year mortality to see if any explanatory variables were predictive of maximum mortality and if/how those variables differed from the prior cases. For the maximum mortality models, cluster was the only random effect grouping factor considered as the repeated measures and temporal components were excluded. Otherwise, model fit and selection followed the process previously described. To further supplement this analysis, we fitted a linear model of maximum mortality by QMD.

The all-years, outbreak years only, and maximum mortality models were cross validated using leave-one-group-out (LOGO) cross validation (125 groups for the all-years and outbreak years only models and 25 groups for the maximum mortality model; Yates et al., 2023) and by calculating mean area under the curve (AUC), root-mean-square-error (RMSE), and log-likelihood values for each model (via the rsample, dplyr, purrr, yardstick, and tibble packages). The final measure of model performance was assessed via accuracy (predicted versus actual mortality) and the Matthews Correlation Coefficient (MCC) (Chicco and Jurman, 2020). We chose to use MCC over the F_1 score or accuracy (ratio of correctly classified to the total number of samples) as MCC is more informative and accurate for assessing binary classifications, particularly for imbalanced datasets (Chicco and Jurman, 2020). We computed MCC scores across a range of five thresholds in increments of 0.05 for each model with starting points informed by the average of predicted probabilities.

Finally, we investigated the influence of each significant variable on the predicted percentage of *P. contorta* killed by *D. ponderosae* by reviewing prediction plots. For each variable, we generated predicted values across all levels of that variable while holding all other variables constant. Given the large number of significant variables and interactions in each of the three models, we imposed a total change threshold whereby we only focus on those variables that produced a $\geq$ 15% change in the predicted probability of mortality across all levels. We acknowledge that our selection of a $\geq$ 15% threshold is somewhat arbitrary and was implemented to streamline the presentation of results. We do not intend to imply that variables that exceeded this threshold are

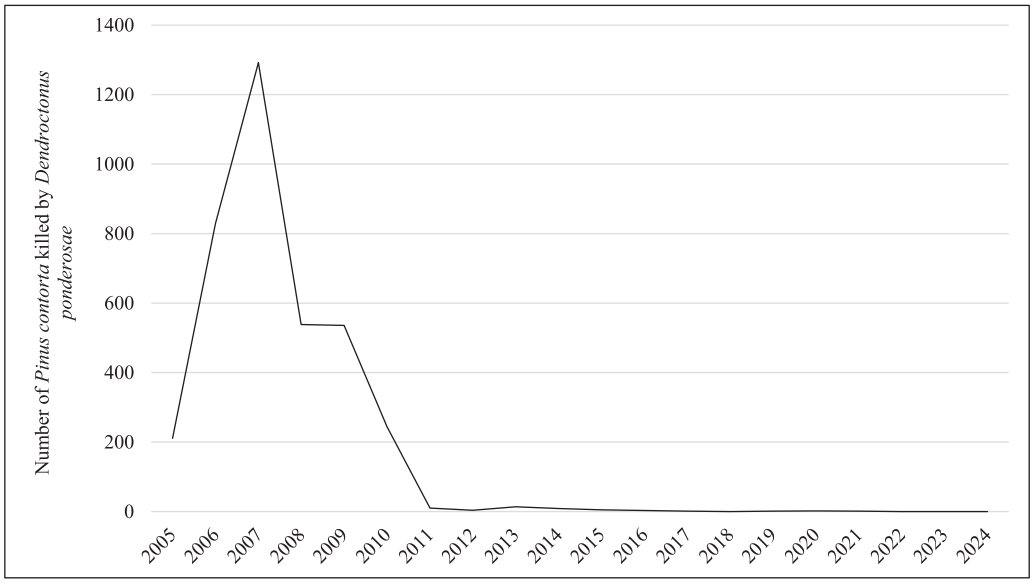

Fig. 1. Total number of *Pinus contorta* killed by *Dendroctonus ponderosae* by year across a network of 125, 0.081-ha circular plots in Colorado, Idaho, Montana, Utah, and Wyoming, U.S., 2005–2024.

necessarily more relevant or important than those that did not.

3. Results

A total of 3957 *P. contorta* was killed by *D. ponderosae* on the plots during 2005–2024 (Fig. 1). The final models fitted to the all-years and outbreak years only datasets converged on the same fixed effects with nearly identical significant variables (Table 2). The only difference between the all-years and outbreaks years only models was average snowpack April-August prior year, which was significant in the outbreak years only model but not in the all-years model. Coefficients, *z*-values, and *P*-values for significant fixed effects are reported in Table 2. Forest plots were generated to show the influence on the odds ratio for *P. contorta* killed by *D. ponderosae* based on each fitted model (Fig. 2). In the all-years model, random effect of plots ($N = 125$) had a variance coefficient of 2.107 and standard deviation of 1.452 and the random effect year ($N = 20$) had a variance coefficient of 5.249 and standard deviation of 2.291. Marginal pseudo R^2 was 0.224 and conditional pseudo R^2 was 0.760. Multicollinearity was low and VIF values for all fixed effects were < 2.74. Mean AUC, RMSE, and log likelihood from LOGO cross validation were 0.905, 0.187, and −11,262, respectively. Model prediction accuracy was 0.867 (95% C.I. = 0.865–0.867) and the MCC was 0.415 at a threshold of 0.20. Results suggested a strong fit and relatively good predictive performance of the fitted all-years model.

In the outbreak years only model, random effect variance coefficients were 2.897 with standard deviation of 1.702 for plots ($N = 125$) and 1.176 with standard deviation of 1.084 for year ($N = 8$). Marginal pseudo R^2 was 0.334 and conditional pseudo R^2 was 0.702 and the model had low multicollinearity; all VIF values were < 2.24. Like observed for the all-years model, LOGO cross validation and MCC values indicate strong fit and relatively good performance for the outbreak years only model with mean AUC of 0.852, mean RMSE of 0.245, mean log likelihood of −10954.26, accuracy of 0.887 (95% C.I. = 0.885–0.889), and MCC of 0.243 with a threshold of 0.15.

Water storage (WS) April-August prior yr, *D. ponderosae* pressure, QMD, individual tree dbh * WS April–August prior yr, and total number of stems ha^{-1} * WS April-August prior yr were the only fixed effects not significant in the maximum mortality model. Coefficients, *z*-values, and *P*-values for all significant fixed effects are reported in Table 3 and the influence of each fixed effect on the odds ratios of *P. contorta* killed by *D. ponderosae* are found in Fig. 3.

The random effect cluster ($N = 25$) had a variance coefficient of 0.823 and a standard deviation of 0.907. While the fixed effects explained slightly more variance in the maximum mortality model than the previous models, the conditional model explained less, marginal pseudo R^2 was 0.385 and conditional pseudo R^2 was 0.508. Once again collinearity was not an issue and all VIF values were < 2.36. Mean AUC, RMSE, and log likelihood from LOGO cross validation was 0.827, 0.363, and −11,078.26, respectively. Model accuracy was 0.786 (95% C.I. = 0.778–0.794) and MCC was 0.449. As observed for the all-years and outbreak years only models, results suggested a strong fit and adequate performance of the maximum mortality model.

Following model fitting, we investigated the influence of each significant variable on the predicted percentage of *P. contorta* killed by *D. ponderosae* by reviewing prediction plots. A summary of the total percentage change estimated from each plot is found in Table 4. We have only included the results from the all-years and maximum mortality models given similarities between the all-years and outbreak years only models reported above. We have included the most influential prediction plots for the all-years (Fig. 4) and maximum mortality models (Fig. 5) using a threshold of $\geq$ 15% change (Table 4).

Although QMD was not a significant fixed effect in the maximum mortality model (unlike in the all-years and outbreak years only models), dbh was among the most significant explanatory variables. This coupled with early data investigation and modeling attempts using proportions of *D. ponderosae*-killed *P. contorta* prompted us to run a simple linear regression on maximum, proportional mortality by QMD, per plot. Mean dbh of all trees and of *P. contorta* were among several other variables fitted but none fit as well as QMD (Fig. 6). Adjusted R^2 was 0.55, $F = 153.7$ (df = 1, 124), and $P < 0.001$. Pearson's product-moment correlation was 0.744, indicating both a significant model fit and strong linear correlation between QMD and the proportion of *P. contorta* killed by *D. ponderosae*. Observed maximum proportions of *P. contorta* killed by *D. ponderosae* for each of the 125 plots with the fitted regression are displayed in Fig. 6.

4. Discussion

We identified several likely drivers of the probability of *P. contorta* mortality attributed to *D. ponderosae* (Table 2). In general, fitted models confirmed our hypotheses of strong, positive relationships between tree dbh and *P. contorta* mortality. Dbh and QMD had the strongest influences on the odds ratios for the all-years and outbreak years only models (Fig. 2). The predicted values curve from the all-years fitted model indicated > 90% probability of mortality for the largest diameter *P. contorta* in the dataset (Fig. 4a). QMD similarly influenced the predicted probability (Fig. 4B). We were surprised at the consistency in fixed effects among the cases of the dataset, particularly between the outbreak years and all-years models. Our expectation was the long observation period following the outbreaks where few beetle-killed *P. contorta* were observed would dampen the influence of several factors; however, they remained largely consistent.

Table 2
Variables significantly correlated with the probability of *Pinus contorta* mortality attributed to *Dendroctonus ponderosae* from 124,584 (all-years model) and 66,522 (outbreak years only model) observations in the Intermountain West, U.S. The all-years model included observations from 2005 to 2025 and the outbreak years only model included observations from 2005 to 2012. Coefficients, *z*-, and *P*-values were generated from fitted generalized linear mixed effects models.

	All-years model			Outbreak years only model		
Fixed Effects	Coefficient	*z*-value	*P*-value	Coefficient	*z*-value	*P*-value
Quadratic mean diameter (QMD)	0.816	18.604	< 0.001	1.024	20.67	< 0.001
Average annual temp. prior yr	−0.34	−3.689	< 0.001	−0.469	−3.896	< 0.001
Dendroctonus ponderosae pressure	0.146	8.288	< 0.001	0.186	7.831	< 0.001
Basal area (BA) ha^{-1}	0.634	8.131	< 0.001	0.739	8.564	< 0.001
Average precipitation Apr-Aug prior yr	0.485	4.22	< 0.001	0.322	4.396	< 0.001
Average snowpack Apr-Aug prior yr	na	na	na	−0.098	−2.126	0.034
Average snowpack Nov-Mar	−0.411	−4.89	< 0.001	−0.244	−4.369	< 0.001
Tree diameter at breast height (dbh)	0.812	28.019	< 0.001	0.942	31.249	< 0.001
Tree height	0.227	6.276	< 0.001	0.211	5.522	< 0.001
Number of nonhost trees ha^{-1}	−0.247	−9.394	< 0.001	−0.457	−6.225	< 0.001
BA ha^{-1} * Average precipitation Apr-Aug prior yr	−0.116	−2.144	0.032	−0.072	−2.302	0.021
BA ha^{-1} * Average snowpack Apr-Aug prior yr	−0.153	−4.642	< 0.001	−0.124	−4.393	< 0.001
Tree dbh * Average precip. Apr-Aug prior yr	−0.104	−2.894	0.004	−0.08	−3.771	< 0.001
Tree dbh * Average snowpack Nov-Mar	−0.115	−3.658	< 0.001	−0.111	−4.522	< 0.001

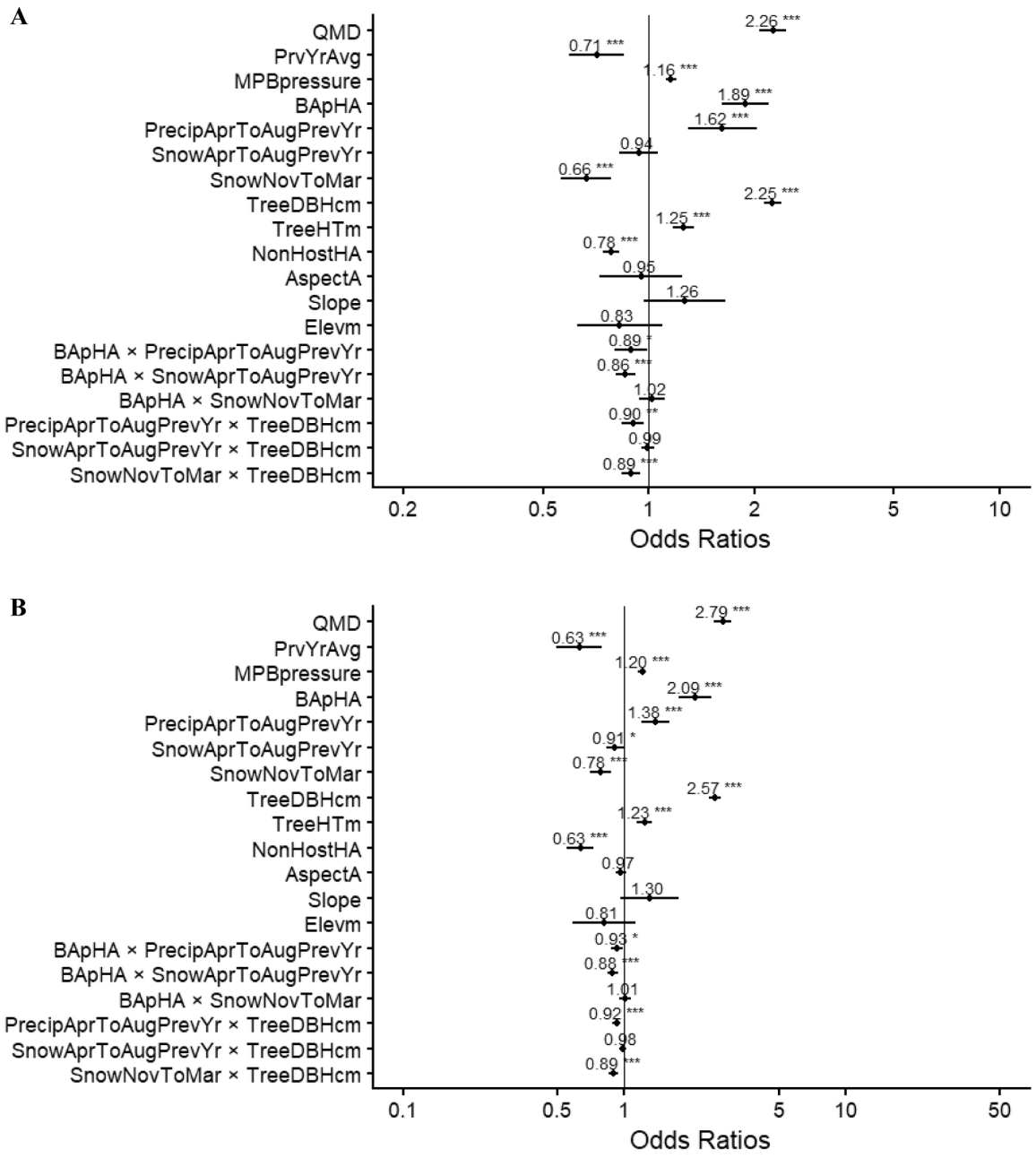

Fig. 2. Forest plots of fixed effects retained in the final fitted all-years (A) and outbreak years only (B) generalized linear mixed effects models. The all-years model included observations from 2005 to 2024 and the outbreak years only model included observations from 2005 to 2012. Estimate (values) and 95% confidence intervals (horizontal lines) of the odds ratio associated with each fixed effect in the models. Asterisks indicate significant values ($\alpha = 0.05$).

Similarly to the all-years and outbreak years only models, there was a strong positive relationship between dbh and mortality for the fitted maximum mortality model (Table 5, Fig. 3, Fig. 5). Interestingly, QMD was not significant in the maximum mortality model. It appears that any correlation between QMD and *P. contorta* mortality was overshadowed by other factors in the maximum mortality model. For instance, the tight 95% C.I. around the predicted values curve may indicate that individual tree dbh accounted for most of the variation in the data available to tree size variables. The probability of mortality approached 100% for the largest dbh *P. contorta* in the maximum mortality model, which agrees with earlier literature on host susceptibility (Shepherd, 1966; Rasmussen, 1972; Thompson, 2017). The fitted linear regression of plot-level proportion of *P. contorta* killed by *D. ponderosae* (Fig. 6) further emphasized the influence of *P. contorta* dbh on the probability of *P. contorta* mortality.

Tree density and water stress are commonly associated with bark beetle activity including for *D. brevicomis* and *D. ponderosae* in *P. ponderosa* (Koontz et al., 2021; Hansen et al., 2023), *Ips* spp. in *P. ponderosa* (Negrón et al., 2009), *Ips* spp. in pinyon pine, *P. edulis* Engelm. (Gaylord et al., 2013), and *D. rufipennis* (Kirby) in *Picea* spp. (DeRose and Long, 2014; Hart et al., 2017). Furthermore, Francis et al. (2025) reported strong, positive correlations between host tree basal area and tree mortality for eight bark beetles including: *D. ponderosa*, *D. brevicomis, D. rufipennis,* Douglas-fir beetle, *D. pseudotsugae* Hopkins, Jeffrey pine beetle, *D. jefferyi* Hopkins, western balsam bark beetle, *Dryocoetes confusus* Swaine, pinyon ips, *Ips confusus* (LeConte), and fir engraver, *Scolytus ventralis* LeConte. As such, we were surprised there were not stronger signals from tree density or water stress variables in our models. Moreover, the direction of the effects was often (but not always) in agreement with our hypotheses, but the strength was often

Table 3
Variables significantly correlated with the probability of *Pinus contorta* mortality attributed to *Dendroctonus ponderosae* from 9766 observations (maximum mortality model) of the highest per year mortality per plot in the Intermountain West, U.S. Coefficients, *z*-, and *P*-values were generated from fitted generalized linear mixed effects model.

Fixed effects	Coefficient	*z*-value	*P*-value
Tree diameter at breast height (dbh)	1.435	34.69	< 0.001
Water storage (WS) Nov-Mar	0.266	3.65	< 0.001
Number of nonhost trees ha^{-1}	−1.542	−3.81	< 0.001
Number of trees ha^{-1}	−3.635	−5.31	< 0.001
Average annual temperature previous yr	−1.892	−2.33	0.02
Aspect	−0.095	−2.2	0.03
Slope	0.127	2.61	0.009
Elevation	0.443	2.24	0.025
Tree dbh * WS Nov-Mar	−0.177	−4.59	< 0.001
Number of trees ha^{-1} * WS Nov-Mar	−0.325	−4.83	< 0.001

much less. For example, basal area ha^{-1} had a strong positive influence on the odds ratios in the all-years and outbreak years only models (Fig. 2) but only accounted for a 1% total change in the probability of *P. contorta* mortality (Table 4). As expected, average precipitation April-August of the prior year and mean snowpack November-March had strong negative influences on the odds ratio, but neither accounted for > 1% total change in the probability of *P. contorta* mortality (Table 4). Average precipitation April-August the prior year and average snowpack November-March both significantly interacted with dbh and QMD (Fig. 4C, D). For the largest dbh *P. contorta*, increased average precipitation April-August the prior year and increased average snowpack November-March decreased the predicted probability of *P. contorta* mortality by ~75 and ~95%, respectively, for the largest dbh *P. contorta* (Table 4).

Pinus contorta is a relatively drought tolerant species (Lotan and Critchfield, 1990) and the influence of water stress on *P. contorta* mortality attributed to *D. ponderosae* is likely less than in some other bark beetle-host tree systems, including *D. ponderosae* in *P. ponderosa*. Kolb et al. (2016) found that severe drought resulted in significantly elevated bark beetle impacts but that moderate drought resulted in notably reduced impacts. Average annual precipitation for *P. contorta* forests in the western U.S. is ~250 mm (Lotan and Critchfield, 1990). Average annual precipitation among our plots during the outbreak years (2005–2012) was 103–324 mm yr^{-1}. The lowest annual precipitation was 16 mm (Utah plot in 2009) and the highest was 598 mm (Colorado plot in 2005) indicating a large amount of variability across the range of our plots.

Number of trees ha^{-1} and water storage November-March both strongly influenced odds ratios in the maximum mortality model, but in the opposite direction than anticipated. Trees ha^{-1} had an inverse relationship with odds of *P. contorta* mortality (Fig. 3), which may be explained by several plots with high numbers of small dbh *P. contorta*. For example, some plots in Utah had 100–250 *P. contorta* (1234–3086 *P. contorta* ha^{-1}), the highest numbers among all plots, but the average dbh of *P. contorta* on these plots were among the lowest (14.0–17.8 cm). As previously indicated, *D. ponderosae* prefers colonizing large-diameter, mature *P. contorta* (Graf et al., 2012). Small-diameter *P. contorta* are poor hosts, a function of reduced phloem thickness, and produce few brood adults (Amman, 1972). The interaction plot for tree diameter and water storage indicated that the highest and lowest levels of water storage in November-March corresponded with low probability of mortality for smaller-diameter *P. contorta* (Fig. 5D), but that the high probability of mortality in larger-diameter trees likely overwhelmed the expected negative influence of water storage on the probability of mortality. Buonanduci et al. (2020) reported clear, opposing influences of stand density for large and small dbh trees, where stand density was positively correlated with the probability of mortality for larger trees but negatively correlated with the probability of mortality for smaller trees. Seasonal water storage significantly interacted with trees ha^{-1}, particularly for the lowest tree densities in the dataset. Predicted probability of mortality in low density plots decreased ~17% across increasing levels of water storage April-August prior year (Table 4, Fig. 5F). Interestingly, the prediction plot for the interaction between November-March water storage and low density indicated a ~70% increase in the probability of *P. contorta* mortality (Table 4., Fig. 5E). This correlation is counter to what we expected as, in general, increased water storage or water availability improves conditions for tree growth and defense (Kolb et al., 2016), particularly in lower density plots given reduced levels of tree competition.

The presence of nonhost trees was a significant factor in all three models (Tables 2 and 3) but did not meet the percent-change threshold from the prediction plots, accounting for ~4% decrease in the all-years model and 10% decrease in the maximum mortality model (Table 4). Increased plant diversity has been demonstrated to reduce insect herbivory in forestry and agriculture (Jactel and Brokerhoff, 2007; Pickett

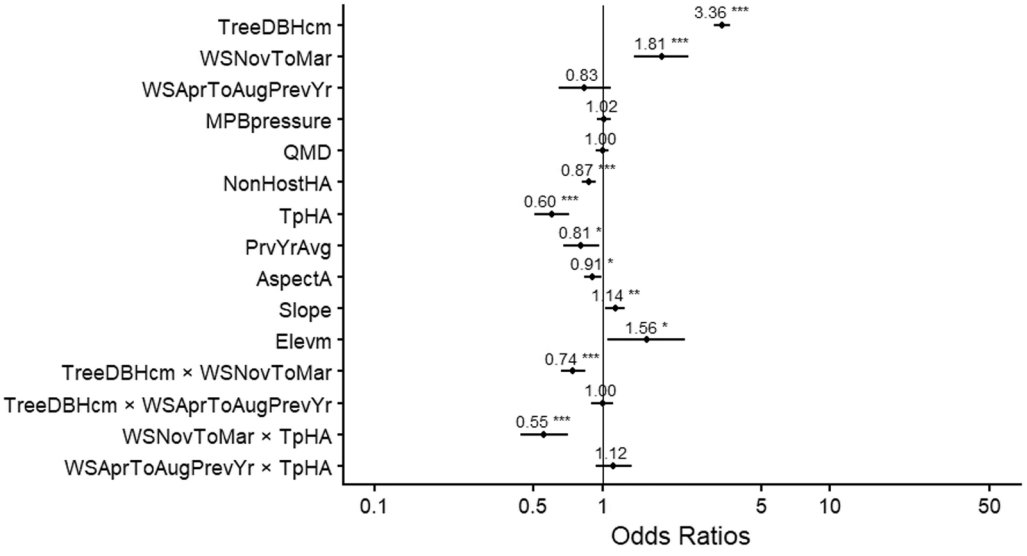

Fig. 3. A forest plot of fixed effects retained in the final fitted maximum mortality generalized linear mixed effects model, which included observations of each plot's highest year of mortality. Estimate (values) and 95% confidence intervals (horizontal lines) of the odds ratio associated with each fixed effect in the models. Asterisks indicate significant values ($\alpha = 0.05$).

Table 4
Significant fixed effects from the all-years and maximum mortality fitted generalized linear mixed effects models and the estimated total change of predicted probabilities of mortality in the Intermountain West, U.S. The all-years model included observations from 2005 to 2025 and the maximum mortality was restricted to the maximum per year mortality per plot.

Fixed Effects	% Change Pred. Plot[a]
All-years model	
Largest tree dbh * increasing levels of average snowpack Nov-Mar	**~95% decrease**
Smallest dbh * increasing levels of average snowpack Nov-Mar	no change
Increasing quadratic mean diameter (QMD)	**~90% increase**
Increasing tree diameter at breast height (dbh)	**~90% increase**
Largest Tree dbh * average precipitation Apr-Aug prior yr	**~75% decrease**
Smallest dbh * increasing levels of average precipitation	~1% decrease
Lowest average snowpack Apr-Aug previous yr * increasing basal area (BA) ha^{-1}	~1.5% increase
Highest average snowpack Apr-Aug previous yr * increasing BA ha^{-1}	no change
Number of nonhost trees ha^{-1}	~4% decrease
All levels of BA ha^{-1} * increasing levels of average precipitation Apr-Aug prior yr	~1% increase both
BA ha^{-1}	~1% increase
Increasing average precipitation Apr-Aug previous yr	~1% decrease
Increasing average annual temp. previous yr	< 1% decrease
Increasing *Dendroctonus ponderosae* pressure	< 1% increase
Tree height	< 1% increase
Increasing average snowpack Nov-Mar	< 1% decrease
Maximum mortality model	
Lowest and highest tree dbh * increasing water storage (WS) Nov-Mar	**~99% increase**
Increasing tree dbh	**~99% increase**
Lowest number of trees ha^{-1} * increasing WS Nov-Mar	**~70% increase**
Highest number of trees ha^{-1} * increasing WS Nov-Mar	~10% decrease
Lowest number of trees ha^{-1} * increasing WS Apr-Aug prior yr	**~25% decrease**
Highest number of trees ha^{-1} * increasing WS Apr-Aug prior yr	~1% increase
Increasing WS Nov–Mar	**~15% increase**
Increasing number of trees ha^{-1}	**~15% decrease**
Increasing average annual temp. previous yr	~11% decrease
Increasing number of nonhost trees ha^{-1}	~10% decrease
Increasing elevation	~10% increase
Increasing WS Apr-–Aug prior yr	~5% decrease
Increasing slope	~5% increase
Increasing aspect	~2% decrease
Increasing *Dendroctonus ponderosae* pressure	~1% increase
Increasing QMD	no change

[a]Total percent change over each variable of predicted values generated from the fitted models. Bold values indicate total change of ≥15%.

et al., 2014; Jactel et al., 2021). Several hypotheses have been postulated to explain this relationship, including resource concentration (host abundance) and host apparency. Zhang and Schlyter (2003) argued that host apparency may be reduced by an increased diversity of semiochemical cues (host and nonhost volatiles) in more diverse forests. To that end, while *P. contorta* remains the dominant tree species in our study, the number of subalpine fir, *Abies lasiocarpa* (Hooker) Nuttall, a nonhost tree species, seedlings and saplings significantly increased (Audley et al., 2020). Total understory cover and cover of shrubs and graminoids (nonhosts) remained unchanged, while cover of forbs (nonhosts) significantly increased (Runyon et al., 2020). Given the overwhelming dominance of *P. contorta* on our plots (mean = 91% in 2005), the fact that we observed a significant nonhost signal in our models suggests there could be an even stronger nonhost effect in more diverse forests. As such, further study of the effects of variation in tree composition is warranted. Of note, volatiles from some nonhosts have been shown to inhibit responses of *D. ponderosae* and other bark beetles to baited traps and trees (Huber et al., 2021).

Perhaps the most surprising result was the negative relationship between higher average temperature in the prior year and *P. contorta* mortality (Figs. 2 and 3). Preisler et al. (2012) also reported a similar relationship for *D. ponderosae* populations in Oregon versus those in Washington and concluded that warming has a relative influence whereby in already warmer areas, beetle populations respond differently than those from cooler areas. Warmer temperatures can accelerate bark beetle development, in some cases even increasing voltinism; reduce overwintering mortality of bark beetles; and increase stress in host trees making them more susceptible to bark beetle colonization (Bentz and Jönson, 2015). Overall, we expected to see a positive relationship between temperature and *P. contorta* mortality but acknowledge that evolved adaptations in *D. ponderosae* serve to synchronize cohorts and minimize the occurrence of cold-sensitive life stages in winter (Bentz et al., 2010). These adaptations may reduce the capacity of *D. ponderosae* to take full advantage of warming, for example limiting the capacity for increases in voltinism (Bentz et al., 2014). The negative relationship in the all-years model resulted in < 1% change from the prediction plots (Table 4). This may indicate our temperature variables did not capture the full influence of temperature specific to this system and may be explained by relatively similar temperatures within a plot and clusters of plots through the duration of the study. We did observe a greater influence of temperatures in the maximum mortality model with a ~11% change (Table 4); however, the snap-shot-in-time nature of this model may be inflating this value. Alternatively, there may be confounding factors we failed to account for in our approach. Furthermore, precipitation and temperature stressors on tree vigor may initiate *D. ponderosae* outbreaks; however, once initiated, host availability and host condition are of greater importance in maintaining an outbreak (Hicke and Jenkins, 2008; Chapman et al., 2012; Creeden et al., 2014; Cooke et al., 2026).

Some counterintuitive results may be an artifact of our plot selection criteria, which focused on forests affected by *D. ponderosae* outbreaks. For example, average basal area across all plots in 2005 was 36.1 m^2 ha^{-1}, well above the < 27.5 m^2 ha^{-1} recommended for reducing susceptibility to *D. ponderosae* in *P. contorta* (Mata et al., 2003). Observations from lower densities in these datasets are really observations following density decreases as a result of *D. ponderosae* activity and should not be considered in the same way as plots that had lower densities prior to *D. ponderosae* outbreaks. A weakness of our dataset is a lack of observations from a broader range of pre-outbreak basal areas.

Another weakness of this study was the number of plots lost resulting in missing observations. It is possible these missing observations could explain some of the unexpected results; however, only five plots were lost prior to 2012. Thus, most of the lost observations occurred during the post-outbreak period when very few *P. contorta* were killed by *D. ponderosae* (Fig. 1). Another possible source of error may have arisen from miscategorized year-of-death resulting from back-dating mortality at plot installation. Given the importance of temporal correlation inherent in this dataset and modeling approach, miscategorized trees may have produced erroneous results. Finally, the geographic spread of these data, a noted strength of this study, may also be a weakness. Spatial variation among plot locations may have introduced too much variability, limiting the ability of our models to reveal some relevant correlations.

Overall model fit and performance was adequate to good for each of the models; however, a significant amount of variation remained unexplained. The fixed effects in each of the three models only explained 22% (all-years model) to 39% (maximum mortality model) of the variability in these data. Interestingly, despite the fixed effects in the all-years model explaining the least amount variation, the conditional all-years model explained the greatest amount of variation (76%). The conditional maximum mortality model explained the least (51%) variation among our models. While we are confident that our models offer strong descriptive power for these data, we acknowledge they have less predictive power, indicated in part by relatively low MCC values.

5. Conclusions

The primary drivers of levels of *P. contorta* mortality attributed to *D.*

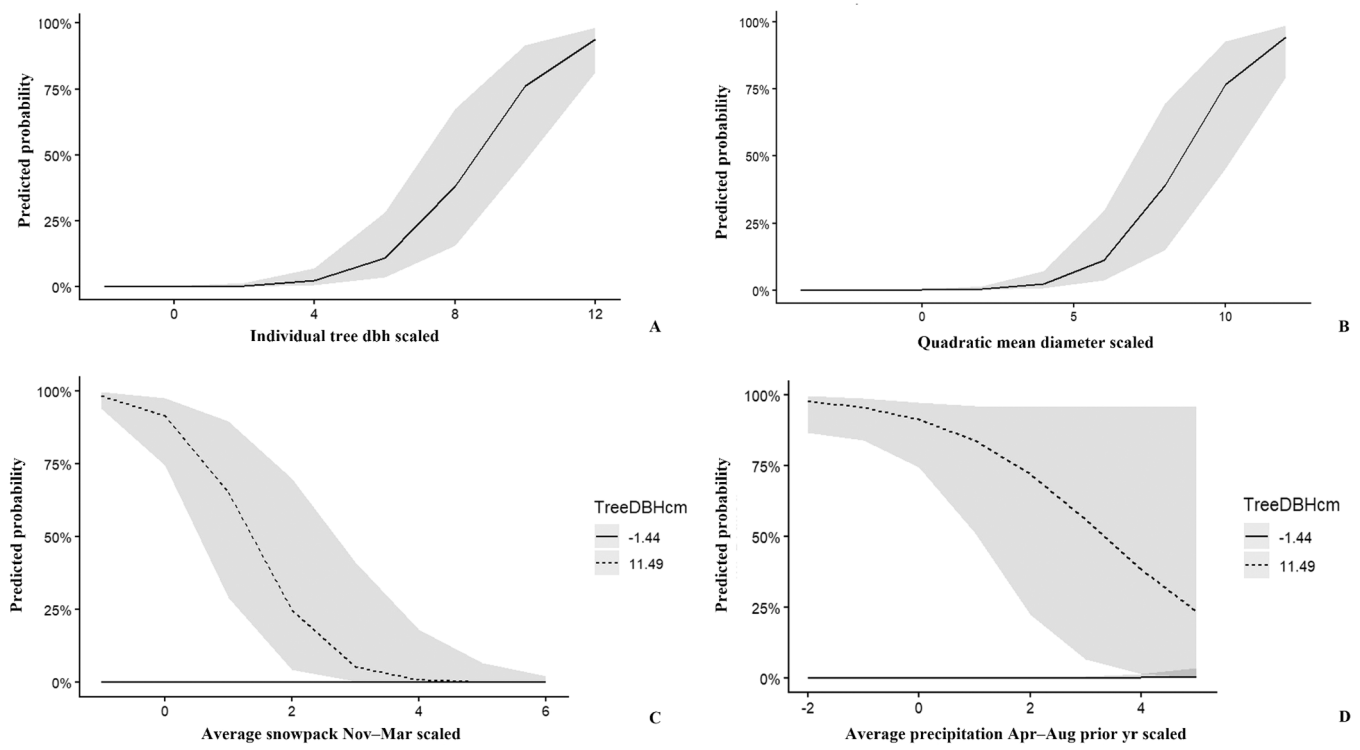

Fig. 4. Prediction plots of the most influential significant fixed effects from the fitted all-years (2005–2024) generalized linear mixed effects model. Prediction curves were generated using predicted values from the final model plotted over the entire range of observed values for each explanatory variable. Interactions include a prediction line for the lowest and highest values for each interaction factor (see legends). Fixed effects include: (A) individual tree diameter at breast height (dbh); (B) quadratic mean diameter (QMD); (C) dbh * average snowpack Nov-Mar; (D) dbh * average precipitation Apr-Aug prior year. Each x-axis displays scaled levels of the explanatory variable.

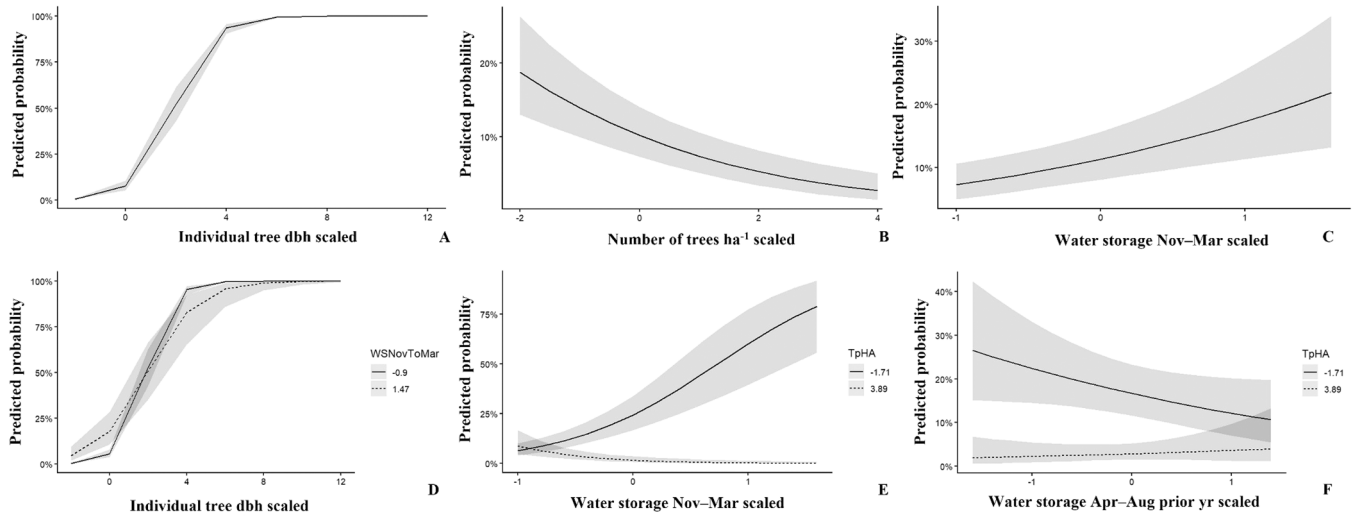

Fig. 5. Prediction plots of the most influential significant fixed effects from the fitted maximum mortality generalized linear mixed effects model, which included observations of each plot's highest year of mortality. Prediction curves were generated using predicted values from the final model plotted over the entire range of observed values for each explanatory variable. Interactions include a prediction line for the lowest and highest values for each interaction factor (see legends). Fixed effects include: (A) individual diameter at breast height (dbh); (B) number of trees ha^{-1}; (C) water storage (WS) Nov-Mar; (D) dbh * WS Nov–Mar; (E) number of trees ha^{-1} * WS Nov-Mar; (F) number of trees ha^{-1} * WS Apr-Aug prior year. Each x-axis displays scaled levels of the explanatory variable.

ponderosae in this study were individual tree dbh and plot-level QMD. Given the well documented preference of *D. ponderosae* for colonizing larger-diameter, mature *P. contorta*, these results were not unexpected. Our models indicated some influences of water availability (as precipitation, snowpack, and water storage); however, overall water stress was not a significant explanatory variable. Our models also indicated tree density (number of trees ha^{-1} or BA) had a positive influence on *P. contorta* mortality while the number of nonhost stems ha^{-1} had a negative influence; though the predicted percent change in mortality was significantly lower than for dbh or QMD. The relatively low importance of tree density is likely the result of the initially high densities across the plot network (Audley et al., 2020) and does not address

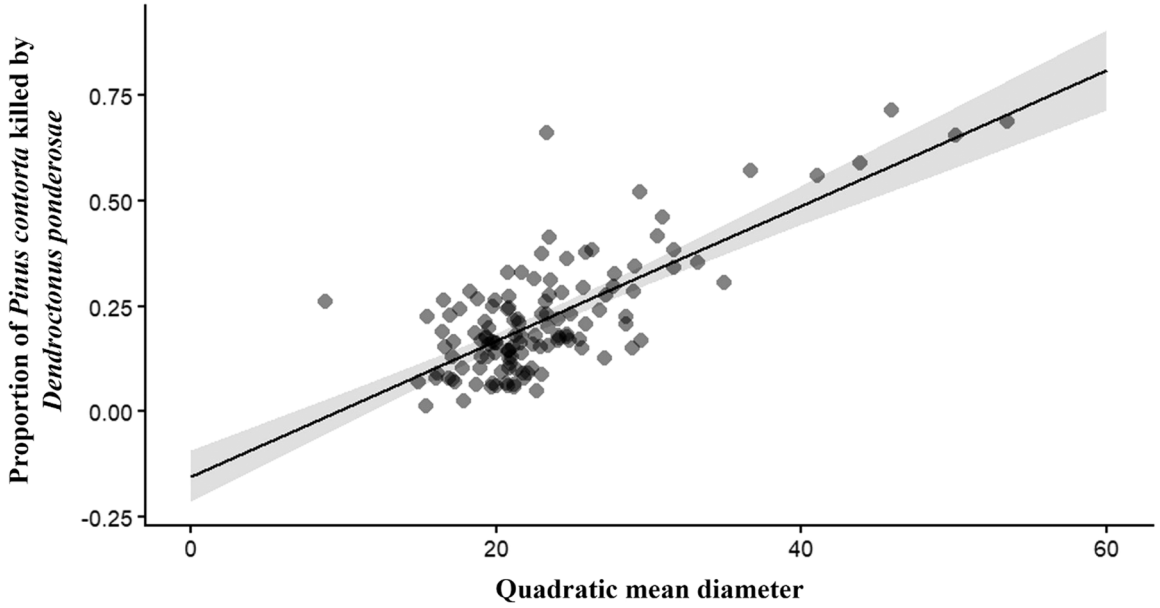

Fig. 6. Linear regression of the highest proportion of *Pinus contorta* killed by *Dendroctonus ponderosae* for each of the 125 0.081-ha circular plots with the fitted regression line and a 95% confidence interval (gray band). The fitted model was significant $F = 153.7$ (df = 1, 124), and $P < 0.001$, with an adjusted $R^2 = 0.55$ and Pearson's product-moment correlation = 0.744.

the effects of lower densities often used in management. Several studies support density management efforts to mitigate the impacts of *D. ponderosae* outbreaks (Safranyik and Wilson, 2006; Whitehead et al., 2007; Fettig et al., 2007). Cooke et al. (2026) reported removal of green trees interrupted the density-dependent feedback and significantly contributed to *D. ponderosae* population collapse. Our results concur and suggest, where possible, forest management should focus on reducing the frequency of large-diameter *P. contorta*. However, with stands of similarly sized trees, or in stands where retention of large-diameter trees is a priority, density reduction and/or increasing tree species (nonhost trees) and structural diversity may provide the best mitigation strategies.

CRediT authorship contribution statement

Jackson P. Audley: Writing – review & editing, Writing – original draft, Visualization, Validation, Methodology, Investigation, Formal analysis, Data curation, Conceptualization. **Andrew M. Latimer:** Writing – review & editing, Writing – original draft, Supervision, Methodology, Investigation, Formal analysis, Conceptualization. **Christopher J. Fettig:** Writing – review & editing, Writing – original draft, Supervision, Resources, Project administration, Methodology, Investigation, Funding acquisition, Conceptualization. **A. Steven Munson:** Writing – review & editing, Investigation, Conceptualization. **Justin B. Runyon:** Writing – review & editing, Investigation, Conceptualization. **Leif A. Mortenson:** Writing – review & editing, Investigation, Data curation. **Brytten E. Steed:** Writing – review & editing, Investigation, Conceptualization. **Kenneth E. Gibson:** Writing – review & editing, Investigation, Conceptualization. **Carl L. Jørgensen:** Writing – review & editing, Investigation, Conceptualization. **Stephen R. McKelvey:** Writing – review & editing, Investigation, Conceptualization. **Joel D. McMillin:** Writing – review & editing, Investigation, Conceptualization. **José F. Negrón:** Writing – review & editing, Investigation, Conceptualization.

Declaration of Competing Interest

The authors declare that they have no known competing financial interests or personal relationships that could have appeared to influence the work reported in this paper.

Acknowledgments

We thank the Arapaho-Roosevelt, Beaverhead-Deerlodge, Boise, Bridger-Teton, Salmon-Challis, and Uinta-Wasatch-Cache National Forests and Grand Teton National Park for their support. This research was funded, in part, by grants from the USDA Forest Service Forest Health Monitoring Program (INT-EM-F−10–03, INT-EM-F−14–01, and INT-EM−17–01 to the Pacific Southwest Research Station), USDA Forest Service Forest Health Protection Regions 1 & 4, and the USDA Forest Service Western Wildland Environmental Threat Assessment Center (24-CS−11272122–041 from the Pacific Southwest Research Station to the University of California, Davis).

Data availability

Data will be made available on request.

References

Amman, G.D., 1972. Mountain pine beetle brood production in relation to thickness of lodgepole pine phloem. J. Econ. Entomol. 65, 138–140. https://doi.org/10.1093/jee/65.1.138.

Audley, J.A., Fettig, C.J., Munson, A.S., et al., 2020. Impacts of mountain pine beetle outbreaks on lodgepole pine forests in the Intermountain West, U.S., 2004–2019. For. Ecol. Manag. 475, 118403. https://doi.org/10.1016/j.foreco.2020.118403.

Bentz, B., Vandygriff, J., Jensen, C., et al., 2014. Mountain pine beetle voltinism and life history characteristics across latitudinal and elevational gradients in the western United States. For. Sci. 60, 434–449. https://doi.org/10.5849/forsci.13-056.

Bentz, B.J., Jönson, A.M., 2015. Modeling bark beetle responses to climate change. In: Vega, F.E., Hofstetter, R.W. (Eds.), Bark beetles. Academic Press, London, pp. 533–553. https://doi.org/10.1016/B978-0-12-417156-5.00013-7.

Bentz, B.J., Régnière, J., Fettig, C.J., et al., 2010. Climate change and bark beetles of the western United States and Canada: Direct and indirect effects. Bioscience 60, 602–613. https://doi.org/10.1525/bio.2010.60.8.6.

Buonanduci, M.S., Morris, J.E., Agne, M.C., et al., 2020. Neighborhood context mediates probability of host tree mortality in a severe bark beetle outbreak. Ecosphere 11 (8). https://doi.org/10.1002/ecs2.3236.

Chapman, T.B., Veblen, T.T., Schoennagel, T., 2012. Spatiotemporal patterns of mountain pine beetle activity in the southern Rocky Mountains. Ecology 93, 2175–2185. https://doi.org/10.1890/11-1055.1.

Chicco, D., Jurman, G., 2020. The advantages of the Matthews correlation coefficient (MCC) over F1 score and accuracy in binary classification evaluation. BMC Genom. 21. https://doi.org/10.1186/s12864-019-6413-7.

Clark, J.S., Iverson, L., Woodall, C.W., et al., 2016. The impacts of increasing drought on forest dynamics, structure, and biodiversity in the United States. Glob. Change Biol. 22, 2329–2352. https://doi.org/10.1111/gcb.13160.
Cooke, B.J., Chubaty, A.M., Carroll, A.L., 2026. The mountain pine beetle in a marginal boreal landscape: Cross-scale collapse triggered by population removal. For. Ecol. Manag. 609, 123645. https://doi.org/10.1016/j.foreco.2026.123645.
Creeden, E.P., Hicke, J.A., Buotte, P.C., 2014. Climate, weather, and recent mountain pine beetle outbreaks in the western United States. For. Ecol. Manag. 312, 239–251. https://doi.org/10.1016/j.foreco.2013.09.051.
DeRose, R.J., Long, J.L., 2014. Resistance and resilience: A conceptual framework for silviculture. For. Sci. 60, 1205–1212. https://doi.org/10.5849/forsci.13-507.
Fettig, C.J., Klepzig, K.D., Billings, R.F., et al., 2007. The effectiveness of vegetation management practices for prevention and control of bark beetle infestations in coniferous forests of the western and southern United States. For. Ecol. Manag. 238, 24–53. https://doi.org/10.1016/j.foreco.2006.10.011.
Fettig, C.J., Asaro, C., Nowak, J.T., et al., 2022. Trends in bark beetle impacts in North America during a period (2000–2020) of rapid environmental change. J. For. 120, 693–713. https://doi.org/10.1093/jofore/fvac021.
Francis, E.J., Jung, C.G., Hicke, J.A., et al., 2025. Modeling the probability of bark beetle-caused tree mortality as a function of watershed-scale host species presence and basal area. For. Ecol. Manag. 580, 122549. https://doi.org/10.1016/j.foreco.2025.122549.
Furniss, R.L., Carolin, V.M., 1977. Western Forest Insects. U.S. Department of Agriculture, Forest Service, Washington, DC.
Gaylord, M.L., Kolb, T.E., Pockman, W.T., et al., 2013. Drought predisposes piñon–juniper woodlands to insect attacks and mortality. New. Phytol. 198, 567–598. https://doi.org/10.1111/nph.12174.
Graf, M., Reid, M.L., Aukema, B.H., et al., 2012. Association of tree diameter with body size and lipid content of mountain pine beetles. Can. Entomol. 144, 467–477. https://doi.org/10.4039/tce.2012.38.
Hansen, E.M., Bentz, B.J., Vandygriff, J.C., et al., 2023. Factors associated with bark beetle infestations of Colorado Plateau ponderosa pine using repeatedly-measured field plots. For. Ecol. Manag. 545, 121307. https://doi.org/10.1016/j.foreco.2023.121307.
Hart, S.J., Veblen, T.T., Schneider, D., et al., 2017. Summer and winter drought drive the initiation and spread of spruce beetle outbreak. Ecology 98, 2698–2707. https://doi.org/10.1002/ecy.1963.
Herms, D.A., Mattson, W.J., 1992. The dilemma of plants: To grow or defend. Quart. Rev. Bio. 67, 283–335. https://www.jstor.org/stable/2830650.
Hicke, J.A., Jenkins, J.C., 2008. Mapping lodgepole pine stand structure susceptibility to mountain pine beetle attack across the western United States. For. Ecol. Manag. 255, 1536–1547. https://doi.org/10.1016/j.foreco.2007.11.027.
Hicke, J.A., Meddens, A.J.H., Kolden, C.A., 2016. Recent tree mortality in the western United States from bark beetles and forest fires. For. Sci. 62, 141–153. https://doi.org/10.5849/forsci.15-086.
Huber, D.P.W., Fettig, C.J., Borden, J.H., 2021. Disruption of coniferophagous bark beetle (Coleoptera: Curculionidae: Scolytinae) mass attack using angiosperm nonhost volatiles: From concept to operational use. Can. Entomol. 153, 19–35. https://doi.org/10.4039/tce.2020.63.
Jactel, H., Brokerhoff, E.G., 2007. Tree diversity reduces herbivory by forest insects. Ecol. Lett. 10, 835–848. https://doi.org/10.1111/j.1461-0248.2007.01073.x.
Jactel, H., Moreira, X., Castagneyrol, B., 2021. Tree diversity and resistance to forest insect pests: Patters, mechanisms, and prospects. Ann. Rev. Entomol. 66, 277–296. https://doi.org/10.1146/annurev-ento-041720-075234.
Klutsch, J.G., Negrón, J.F., Costello, S.L., et al., 2009. Stand characteristics and downed woody debris accumulations associated with a mountain pine beetle (*Dendroctonus ponderosae* Hopkins) outbreak in Colorado. For. Ecol. Manag. 258, 641–649. https://doi.org/10.1016/j.foreco.2009.04.034.
Kolb, T.E., Fettig, C.J., Ayers, M.P., et al., 2016. Observed and anticipated impacts of drought on forest insects and diseases in the United States. For. Ecol. Manag. 380, 321–334. https://doi.org/10.1016/j.foreco.2016.04.051.
Koontz, M.J., Latimer, A.M., Mortenson, L.A., et al., 2021. Cross-scale interaction of host tree size and climatic water deficit governs bark beetle-induced tree mortality. Nat. Commu. 12, 1–13. https://doi.org/10.1038/s41467-020-20455-y.
Lotan, J.E., Critchfield, W.B., 1990. Lodgpole pine. Silvics of North America. U.S. Department of Agriculture, Forest Service. https://research.fs.usda.gov/silvics/lodgepole-pine.
Mata, S.A., Schmid, J.M., Olsen, W.K., 2003. Growth of Lodgepole Pine Stands and Its Relation to Mountain Pine Beetle Susceptibility. RMRS-RP-42. U.S. Department of Agriculture, Forest Service, Rocky Mountain Research Station, Fort Collins, CO, p. 19.
Morris, J.L., Cottrell, S., Fettig, C.J., et al., 2018. Bark beetles as agents of change in social-ecological systems. Fron. Ecol. Environ. 16, S34–S43. https://doi.org/10.1002/fee.1754.
Negrón, J.F., Fettig, C.J., 2014. Mountain pine beetle, a major disturbance agent in US western coniferous forests: A synthesis of the state of knowledge. For. Sci. 60, 409–413. https://doi.org/10.5849/forsci.13-169.
Negrón, J.F., McMillin, J.D., Anhold, J.A., et al., 2009. Bark beetle-caused mortality in a drought-affected ponderosa pine landscape. For. Ecol. Manag. 257, 1353–1362. https://doi.org/10.1016/j.foreco.2008.12.002.
Pickett, J.A., Woodcock, C.M., Midega, C.A., Khan, Z.R., 2014. Push–pull farming systems. Curr. Opin. Biotechnol. 26, 125–132. https://doi.org/10.1016/j.copbio.2013.12.006.
Preisler, H.K., Hicke, J.A., Ager, A.A., Hayes, J.L., 2012. Climate and weather influences on spatial temporal patterns of mountain pine beetle populations in Washington and Oregon. Ecology 93, 2421–2434. https://doi.org/10.1890/11-1412.1.
Raffa, K.F., Berryman, A.A., 1982. Physiological differences between lodgepole pines resistant and susceptible to the mountain pine beetle and associated microorganisms. Environ. Entomol. 11, 486–492. https://doi.org/10.1093/ee/11.2.486.
R Core Team, 2024. R: A language and environment for statistical computing. R Core Team, Vienna, Austria. https://R-project.org/.
Raffa, K.F., Aukema, B.H., Bentz, B.J., et al., 2008. Cross-scale drivers of natural disturbances prone to anthropogenic amplification: The dynamics of bark beetle eruptions. Bioscience 58, 501–517. https://doi.org/10.1641/B580607.
Rasmussen, L.A., 1972. Attraction of mountain pine beetle to small diameter lodgepole pines baited with *trans*-verbenol and alpha-pinene. J. Econ. Entomol. 65, 1396–1399. https://doi.org/10.1093/jee/65.5.1396.
Runyon, J.B., Fettig, C.J., Trilling, J.A., et al., 2020. Changes in understory vegetation including invasive weeds following mountain pine beetle outbreaks. Trees For. People 2, 100038. https://doi.org/10.1016/j.tfp.2020.100038.
Safranyik, L., Wilson, B., 2006. Natural Resources Canada. The Mountain Pine Beetles A Synthesis of Biology, Management, and Impacts on Lodgepole Pine. Canadian Forest Service, Victoria, BC.
Shepherd, R.F., 1966. Factors influencing the orientation and rates of activity of *Dendroctonus ponderosae* Hopkins (Coleoptera: Scolytidae). Can. Entomol. 98, 507–518. https://doi.org/10.4039/Ent98507-5.
Six, D.L., Bracewell, R., 2015. *Dendroctonus*. In: Vega, F.E., Hofstetter, R.W. (Eds.), Bark Beetles. Academic Press, London, pp. 305–350. https://doi.org/10.1016/B978-0-12-417156-5.00008-3.
Thompson, M.T., 2017. Assessing the impact of mountain pine beetle infestation on stand structure of lodgepole pine forests in Colorado using the forest inventory and analysis annual forest inventory. J. For. 115, 270–275. https://doi.org/10.5849/jof.15-057.
Whitehead, R.J., Russo, G.L., Hawks, B.C., Armitage, O.B., 2007. A Silvicultural Assessment of 10 Lodgepole Pine Stands After Partial Cutting to Reduce Susceptibility to Mountain Pine Beetle. Natural Resources Canada. Canadian Forest Service, Victoria, BC.
Yates, L.A., Aandahl, Z., Richards, S.A., et al., 2023. Cross validation for model selection: A review with examples from ecology. Ecol. Monogr. 93, e1557. https://doi.org/10.1002/ecm.1557.
Zhang, Q.H., Schlyter, F., 2003. Redundancy, synergism, and active inhibitory range of non-host volatiles in reducing pheromone attraction in European spruce bark beetle *Ips typographus*. Oikos 101, 299–310. https://doi.org/10.1034/j.1600-0706.2003.111595.x.
Zuur, A., Leno, E., Walker, N., et al., 2009. Mixed effects models and extensions in ecology with R. Springer-Verlag. https://doi.org/10.1007/978-0-387-87458-6.